Acta Cryst. (1996). B52, 287–295

Structure at 200 and 298 K and X-ray Investigations of the Phase Transition at 242 K of $[NH_2(CH_3)_2]_3Sb_2Cl_9$ (DMACA)†

JACEK ZALESKI[a] AND ADAM PIETRASZKO[b]

[a]*Institute of Chemistry, University of Opole, 45-951 Opole, Oleska 48, Poland, and* [b]*Institute of Low Temperature and Structure Research, Polish Academy of Sciences, 50-950 Wroclaw, Okólna 2, Poland*

(*Received 29 December 1994; accepted 26 July 1995*)

Abstract

$[NH_2(CH_3)_2]_3Sb_2Cl_9$ (dimethylammonium nonachlorodiantimonate, DMACA) has, at 200 K, a monoclinic *Pc* space group, with $a = 9.470(3)$, $b = 9.034(3)$, $c = 14.080(4)$ Å, $\beta = 95.81(3)°$, $V = 1198.4(4)$ Å^3, $Z = 2$ [$R = 0.024$, $wR = 0.025$ for 4613 independent reflections with $F > 4\sigma(F)$]. At 298 K DMACA has $P2_1/c$ space group with $a = 9.686(3)$, $b = 9.037(3)$, $c = 14.066(4)$ Å, $\beta = 95.57(3)°$, $V = 1225.3(5)$ Å^3, $Z = 2$ [$R = 0.034$, $wR = 0.035$ for 2736 reflections with $F > 4\sigma(F)$]. The anionic sublattice of DMACA consists of polyanionic $(Sb_2Cl_9^{3-})_n$ layers. In the low-temperature phase there are three crystallographically non-equivalent dimethylammonium cations in the crystal structure. One of the cations is located inside the polyanionic layers, two others – one ordered and one disordered – between the polyanionic layers. In the room-temperature phase there are two non-equivalent cations – both disordered – in the crystal structure. Temperature dependencies of lattice parameters between 200 and 300 K were determined. The occurrence of a second-order phase transition at $T = 242$ K was confirmed. The dependence of lengths of Sb—Cl contacts on the presence and strength of N—H···Cl hydrogen bonds was discussed. It was found that lengths of Sb—Cl bonds may differ from each other by as much as 0.3 Å, because of the presence of N—H···Cl hydrogen bonds. These differences were attributed to distortion of the lone-electron pair on antimony(III).

1. Introduction

Alkylammonium halogenoantimonates are a new family of compounds with polar ferroelectric and pyroelectric properties (Jakubas & Sobczyk, 1990). Of the many different stoichiometries in which these compounds crystallize, the $R_3Sb_2X_9$ subgroup (R = alklyammonium cation, X = Cl, Br or I) has received most attention. These compounds are salts containing molecular ions, their anionic sublattices are built of distorted $SbCl_6^{3-}$ octahedra connected with each other in such a way that three halogen atoms of the coordination sphere of the Sb atom are bridging and three are terminal. Depending on the type of halogen atom and the spatial size of the cations, four different arrangements are possible:

(*a*) isolated units composed of two face-sharing octahedra (Chabot & Parthe, 1978; Hall, Nunn, Begley & Sowerby, 1986; Fig. 1*a*);

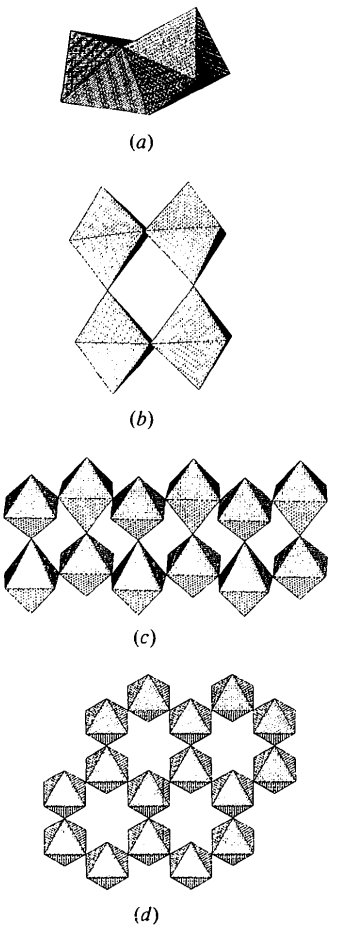

Fig. 1. Comparison of anionic sublattices present in different halogenoantimonates and bismuthates of $R_3M_2X_5$ stoichiometry (R = alkylammonium cation, M = antimony or bismuth, X = chlorine, bromine or iodine), as a polyhedral representation.

† This work was awarded an Oxford Cryosystem award at ECM16 at Lund 1995 for the best low temperature poster.

(*b*) isolated units composed of four octahedra (Aurivillius & Stalhandske, 1978; Fig. 1*b*);

(*c*) polyanionic one-dimensional zigzag chains (Kihara & Sudo, 1971; Jakubas *et al.*, 1986; Fig. 1*c*);

(*d*) polyanionic two-dimensional layers (Lazarini, 1977; Kallel & Batts, 1985; Fig. 1*d*).

The alkylammonium cations are located between the anions and are connected to the halogen atoms by hydrogen bonds. They possess considerable freedom of reorientation in the solid state, which on decreasing temperature is consecutively frozen at phase transitions (Jakubas & Sobczyk, 1990). It was found that the most interesting compounds from the point of view of dielectric properties were those with polyanionic two-dimensional layers. Ferroelectric properties were found in $[NH_2(CH_3)_2]_3Sb_2Cl_9$, DMACA (Jakubas, 1986), $[NH_2(CH_3)_2]_3Sb_2Br_9$, DMABA (Jakubas, Sobczyk & Matuszewski, 1987) and $[NH(CH_3)_3]_3Sb_2Cl_9$, TMACA (Jakubas, Czapla, Galewski & Sobczyk, 1986).

The structure of DMACA was determined at 301 K (space group $P2_1/c$, $a = 9.670$, $b = 9.018$, $c = 14.045$ Å and $\beta = 95.47°$). Two crystallographically non-equivalent DMA cations were found in the unit cell; one disordered and located about a centre of symmetry inside polyanionic cavities, the other located at the general position between the polyanionic layers (Gdaniec, Kosturkiewicz, Jakubas & Sobczyk, 1988).

DMACA undergoes a ferro-paraelectric second-order phase transition at 242 K (Jakubas, 1986) and an irreversible change at 368 K connected probably with decomposition (Galewski, Jakubas & Sobczyk 1990). The mechanism of the ferro-paraelectric transition was attributed to ordering of the dimethylammonium cations located in polyanionic cavities. It was suggested that dynamical reorientations of these cations between two positions are frozen at T_c, which result in the appearance of spontaneous polarization (Jakubas, Malarski & Sobczyk, 1988). The polar properties were found in the *ac* plane, with maximum values of spontaneous polarization along the *c* direction (Miniewicz & Jakubas, 1987). The activation energy estimated from dielectric dispersion studies is 16 kJ mol^{-1}. Critical slowing down of the relaxation frequency within 10 K of T_c was observed in the paraelectric phase (Bator & Jakubas, 1995). The spectroscopic studies revealed continuous changes in the frequencies of Raman bands at 242 K, with no soft mode behaviour (Miniewicz, Lefebvre & Jakubas, 1991).

Two of the anisotropic thermal parameters of the so-called ordered cation were found to be unreasonably large [U_{11} C(2) = 0.31 and U_{33} N(1) = 0.33 (Gdaniec, Kosturkiewicz, Jakubas & Sobczyk, 1988)], suggesting the possibility of some type of disorder in this cation. The goal of the present work is to determine the crystal structure of DMACA in the ferroelectric phase, redetermine its structure in the paraelectric phase and to investigate the phase transition at 242 K by X-ray diffraction.

2. Experimental

$[NH_2(CH_3)_2]_3Sb_2Cl_9$ (DMACA) crystals were obtained as described elsewhere (Jakubas, 1986). Data for structure determination were collected on a KM-4 KUMA diffractometer with Mo$K\alpha$ radiation ($\lambda = 0.71073$ Å, graphite mononochromator). Lattice parameters were refined from setting angles of 26 reflections in the $19 < 2\theta < 30°$ range. The reflections were collected using the ω–θ scan technique (scan speed 0.03–0.15 s^{-1}; scan width 1.5°). Two control reflections measured after intervals of 50 showed negligible intensity variation. Lorentz–polarization and semi-empirical absorption corrections were applied. The *SHELXTL/PC* program (Sheldrick, 1990) was used for all the structure calculations and drawings.

Crystal data for DMACA at 200 and 298 K, together with the measurement parameters, are given in Table 1.

The thermal expansion studies were carried out on a single crystal of DMACA using a KM-4 diffractometer. The lattice parameters were refined from setting angles of 20 reflections in the $19 < 2\theta < 30°$ range. The temperature was controlled using an Oxford Cryosystem cooler (dry-nitrogen gas stream, temperature stability ± 0.1 K).

3. Results and discussion

3.1. *Structure of DMACA*

3.1.1. *At 200 K.* The structure was solved by the Patterson method; a subsequent difference-Fourier synthesis revealed the positions of all non-H atoms. The H atoms were added from geometric considerations. The H atoms of methyl groups were not refined, while the positional and thermal parameters of all other atoms were refined in a full-matrix least-squares method. The resulting positions of H atoms of NH_2 groups were confirmed by difference-Fourier synthesis.

The space group *Pc* was deduced from systematic absences. The choice was unambiguous. It implies the location of a polar vector in the *ac* plane, as shown experimentally in the dielectric studies (Miniewicz & Jakubas, 1987).

Atomic coordinates and equivalent isotropic displacement coefficients for DMACA are given in Table 2 and the interatomic distances and angles in Table 3.

The projection of the crystal structure of DMACA at 200 K in the *a* direction is shown in Fig. 2. Its anionic sublattice is in the form of two-dimensional layers, lying in the *bc* plane, formed by distorted $SbCl_6^{3-}$ octahedra. Six $SbCl_6^{3-}$ octahedra connected by corners form a cavity

Table 1. *Experimental details*

Crystal data		
Chemical formula	$C_6H_{24}Cl_9N_3Sb_2$	$C_6H_{24}Cl_9N_3Sb_2$
Chemical formula weight	700.8	700.8
Cell setting	Monoclinic	Monoclinic
Space group	*Pc*	$P2_1/c$
a (Å)	9.470 (3)	9.686 (3)
b (Å)	9.034 (3)	9.037 (3)
c (Å)	14.080 (4)	14.066 (4)
β (°)	95.81 (3)	95.57 (3)
V (Å^3)	1198.4 (4)	1225.3 (5)
Z	2	2
D_x (Mg m^{-3})	1.942	1.899
Radiation type	Mo $K\alpha$	Mo $K\alpha$
Wavelength (Å)	0.71073	0.71073
No. of reflections for cell parameters	26	26
θ range (°)	9.5–15	9.5–15
μ (mm^{-1})	3.28	3.22
Temperature (K)	200	298
Crystal form	Irregular	Irregular
Crystal size (mm)	0.4 × 0.4 × 0.3	0.4 × 0.4 × 0.3
Crystal colour	Colourless	Colourless
Data Collection		
Diffractometer	Kuma KM-4	Kuma KM-4
Data collection method	ω–θ	ω–θ
Absorption correction	Semi-empirical	None
T_{min}	0.250	–
T_{max}	0.318	–
No. of measured reflections	10 529	8427
No. of independent reflections	5788	4780
No. of observed reflections	4613	2736
Criterion for observed reflections	$F > 4.0\sigma(F)$	$F > 4\sigma(F)$
R_{int}	0.0168	0.0307
θ_{max} (°)	32	40
Range of h, k, l	$-17 \rightarrow h \rightarrow 17$ $-16 \rightarrow k \rightarrow 16$ $0 \rightarrow l \rightarrow 15$	$-15 \rightarrow h \rightarrow 15$ $-14 \rightarrow k \rightarrow 14$ $0 \rightarrow l \rightarrow 17$
No. of standard reflections	2	2
Frequency of standard reflections	Every 50 reflections	Every 50 reflections
Intensity decay (%)	Negligible	Negligible
Refinement		
Refinement on	F	F
R	0.0241	0.0336
wR	0.0252	0.0347
S	0.95	1.26
No. of reflections used in refinement	4613	2736
No. of parameters used	233	133
Data:parameter ratio	19.8:1	20.6:1
H-atom treatment	H atoms were placed in calculated positions; methyl H atoms were not refined, positional and displacement parameters for all others were refined	H atoms were placed in calculated positions and were not refined
Weighting scheme	$w^{-1} = \sigma^2(F) + 99F^2$	$w^{-1} = \sigma^2(F) + 99F^2$
$(\Delta/\sigma)_{max}$	0.086	0.201
$\Delta\rho_{max}$ (e Å^{-3})	0.81	0.72
$\Delta\rho_{min}$ (e Å^{-3})	−0.50	−0.92
Extinction method	None	None
Source of atomic scattering factors	*SHELXTL/PC* (Sheldrick, 1990)	*SHELXTL/PC* (Sheldrick, 1990)

inside the polyanionic layer. The cavities have shapes of a cube truncated on two sides perpendicular to the C_3 axis. One of the crystallographically non-equivalent cations N(1) is located inside the polyanionic cavities, while two others are located between the layers. The cations are connected to Cl atoms by N—H···Cl hydrogen bonds.

One of the cations located between the layers is disordered. The disorder is realized by splitting the N and C atoms between two positions with occupancy factors of 0.73 for N(31), C(51) and C(61), and 0.27 for N(32), C(52) and C(62).

3.1.2. *At 298 K.* The structure was solved by the Patterson method and subsequent difference-Fourier synthesis. H atoms were added from geometric considerations. They were not refined since they were not visible on a difference-Fourier synthesis.

Atomic coordinates and equivalent isotropic displacement coefficients for DMACA at 298 K are given in Table 4.

Table 2. *Fractional atomic coordinates and equivalent isotropic displacement parameters ($Å^2$) for DMACA at 200 K*

$$U_{eq} = (1/3)\Sigma_i\Sigma_j U_{ij} a_i^* a_j^* \mathbf{a}_i.\mathbf{a}_j.$$

	x	y	z	U_{eq}
Sb(1)	0.0	0.2102	0.0	0.026 (1)
Sb(2)	0.3245 (1)	0.7043 (1)	0.1687 (1)	0.025 (1)
Cl(1)	0.4541 (2)	0.5329 (2)	0.2758 (1)	0.041 (1)
Cl(2)	−0.1457 (2)	0.0217 (2)	−0.0809 (2)	0.048 (1)
Cl(3)	−0.1830 (2)	0.3923 (2)	−0.0523 (2)	0.041 (1)
Cl(4)	0.1925 (2)	−0.0347 (2)	0.0490 (1)	0.045 (1)
Cl(5)	0.4571 (2)	0.6554 (2)	0.0363 (1)	0.041 (1)
Cl(6)	−0.1279 (2)	0.1663 (2)	0.1514 (1)	0.042 (1)
Cl(7)	0.5227 (2)	0.8972 (2)	0.2224 (2)	0.043 (1)
Cl(8)	0.1564 (2)	0.4853 (2)	0.1083 (1)	0.044 (1)
Cl(9)	0.1149 (2)	0.7617 (2)	0.3338 (1)	0.055 (1)
N(1)	0.1172 (5)	−0.1801 (5)	−0.1609 (4)	0.049 (1)
C(1)	0.2497 (7)	−0.1668 (8)	−0.2039 (6)	0.056 (1)
C(2)	0.0837 (9)	−0.3313 (8)	−0.1333 (6)	0.072 (1)
N(2)	−0.1883 (5)	0.6972 (5)	0.2070 (4)	0.046 (1)
C(3)	−0.2025 (6)	0.5350 (6)	0.1969 (4)	0.041 (1)
C(4)	−0.1548 (6)	0.7667 (7)	0.1177 (6)	0.063 (1)
N(31)	0.5331 (7)	0.8724 (7)	0.5518 (5)	0.046 (1)
C(51)	0.4941 (9)	0.7371 (9)	0.6001 (9)	0.085 (1)
C(61)	0.5023 (8)	0.8875 (11)	0.4495 (6)	0.074 (1)
N(32)	0.4844 (13)	0.8178 (13)	0.4715 (12)	0.093 (1)
C(52)	0.4512 (13)	0.7150 (13)	0.5392 (12)	0.086 (1)
C(62)	0.5430 (14)	0.9734 (13)	0.4959 (13)	0.102 (1)

Table 3. *Selected geometric parameters (Å, °) for DMACA at 200 K*

Sb(1)—Cl(2)	2.405 (2)	Sb(2)—Cl(9)	3.247 (2)
Sb(1)—Cl(3)	2.447 (2)	N(1)—C(1)	1.45 (1)
Sb(1)—Cl(4)	2.905 (2)	N(1)—C(2)	1.46 (1)
Sb(1)—Cl(6)	2.587 (2)	N(2)—C(3)	1.48 (1)
Sb(1)—Cl(8)	3.199 (2)	N(2)—C(4)	1.47 (1)
Sb(2)—Cl(1)	2.409 (2)	N(31)—C(51)	1.46 (1)
Sb(2)—Cl(5)	2.393 (2)	N(31)—C(61)	1.45 (1)
Sb(2)—Cl(7)	2.617 (2)	N(32)—C(52)	1.39 (2)
Sb(2)—Cl(8)	2.625 (2)	N(32)—C(62)	1.54 (2)
Cl(2)—Sb(1)—Cl(3)	88.8 (1)	Cl(1)—Sb(2)—Cl(9)	87.9 (1)
Cl(2)—Sb(1)—Cl(4)	83.7 (1)	Cl(5)—Sb(2)—Cl(7)	86.0 (1)
Cl(2)—Sb(1)—Cl(6)	89.3 (1)	Cl(5)—Sb(2)—Cl(8)	87.6 (1)
Cl(2)—Sb(1)—Cl(8)	172.5 (1)	Cl(5)—Sb(2)—Cl(9)	174.0 (1)
Cl(3)—Sb(1)—Cl(4)	172.5 (1)	Cl(7)—Sb(2)—Cl(8)	171.4 (1)
Cl(3)—Sb(1)—Cl(6)	88.6 (1)	Cl(7)—Sb(2)—Cl(9)	99.2 (1)
Cl(3)—Sb(1)—Cl(8)	84.3 (1)	Cl(8)—Sb(2)—Cl(9)	87.6 (1)
Cl(4)—Sb(1)—Cl(6)	91.2 (1)	Sb(1)—Cl(8)—Sb(2)	167.3 (1)
Cl(4)—Sb(1)—Cl(8)	103.2 (1)	C(1)—N(1)—C(2)	114 (1)
Cl(6)—Sb(1)—Cl(8)	87.7 (1)	C(3)—N(2)—C(4)	112 (1)
Cl(1)—Sb(2)—Cl(5)	95.5 (1)	C(51)—N(31)—C(61)	121 (1)
Cl(1)—Sb(2)—Cl(7)	86.6 (1)	C(52)—N(32)—C(62)	124 (2)
Cl(1)—Sb(2)—Cl(8)	88.4 (1)		

The projection of the crystal structure of DMACA at 298 K in the *a* direction is shown in Fig. 3 to facilitate comparison with the structure at 200 K.

The positions of Sb and Cl atoms, together with the values of their temperature factors, were as previously determined (Gdaniec, Kosturkiewicz, Jakubas & Sobczyk, 1988). The only differences result from assuming a different model for the cationic sublattice. In previous work, out of two non-equivalent cations, one located in polyanionic cavities was disordered by splitting the N atom between the two positions with an occupancy factor 0.5. The other cation was found to be ordered. In our model we split the N and C atoms of the first cation with an occupancy factor 0.5 (Fig. 4*a*). By assuming that the second cation is ordered, we have obtained very large anisotropic temperature factors for N(2) and C(3). Better results were, however, obtained by splitting N(2) between three positions N(21), N(22) and N(23), with occupancy factors 0.48, 0.37 and 0.15, respectively. Accordingly, C(3) was also split between two positions, C(31) and C(32), with occupancy factors 0.85 and 0.15, respectively (Fig. 4*b*).

The differences in structure of DMACA at 298 and 200 K have their origin in the disorder of the cationic sublattice and different deformations of the anionic sublattice. These will be discussed in parts II and III, respectively, of the present work.

3.2. *Phase transition at 242 K of DMACA*

The temperature dependence of lattice parameters *a*, *b*, *c* and β for DMACA between 200 and 300 K is shown in Fig. 5.

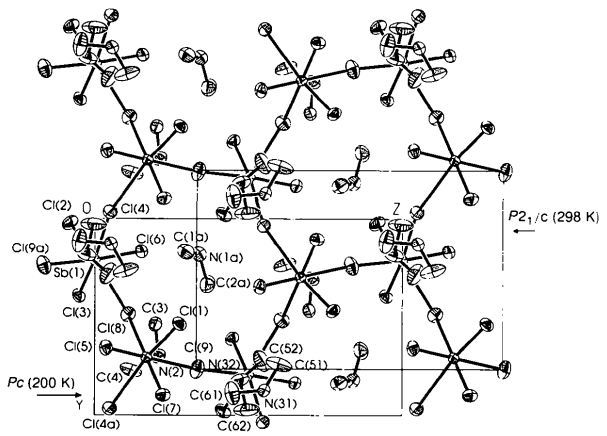

Fig. 2. Projection of the crystal structure of DMACA at 200 K down the *a* axis. Thermal ellipsoids are at 50% probability.

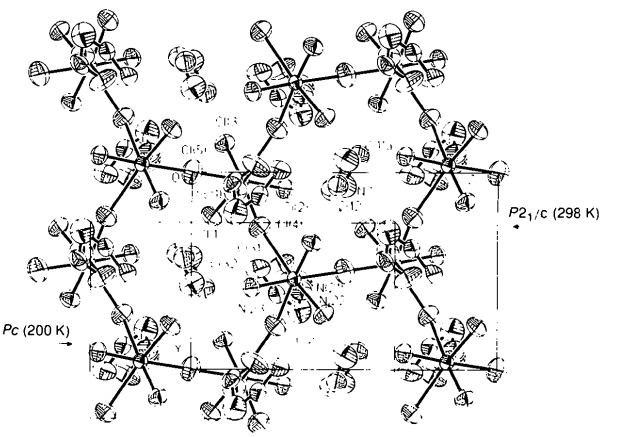

Fig. 3. Projection of the crystal structure of DMACA at 298 K down the *a* axis. Thermal ellipsoids are at 50% probability.

Table 4. *Fractional atomic coordinates and equivalent isotropic displacement parameters (Å²) for DMACA at 298 K*

$$U_{eq} = (1/3)\Sigma_i\Sigma_j U_{ij} a_i^* a_j^* \mathbf{a}_i.\mathbf{a}_j.$$

	x	y	z	U_{eq}
Sb(1)	0.3394 (1)	0.0391 (1)	0.1640 (1)	0.048 (1)
Cl(1)	0.2094 (2)	0.2206 (2)	0.0670 (1)	0.085 (1)
Cl(2)	0.2094 (2)	0.0841 (2)	0.3028 (1)	0.079 (1)
Cl(3)	0.1591 (2)	−0.1467 (2)	0.1062 (1)	0.083 (1)
Cl(4)	0.5170 (2)	0.2755 (2)	0.2235 (1)	0.090 (1)
Cl(5)	1/2	0.0	0.0	0.132 (1)
N(1)	0.4613 (9)	0.0627 (10)	0.4973 (9)	0.121 (1)
C(11)	0.4352 (11)	−0.0824 (11)	0.5367 (10)	0.106 (1)
C(12)	0.6032 (10)	0.0714 (11)	0.4706 (10)	0.098 (1)
N(21)	0.1419 (10)	0.5510 (10)	0.3675 (7)	0.095 (1)
N(22)	0.2207 (10)	0.5976 (11)	0.3572 (9)	0.095 (1)
N(23)	0.1470 (13)	0.6183 (13)	0.2818 (12)	0.081 (1)
C(2)	0.1256 (7)	0.7005 (8)	0.3548 (5)	0.119 (1)
C(31)	0.1900 (8)	0.4693 (9)	0.2913 (7)	0.133 (1)
C(32)	0.1792 (13)	0.4916 (13)	0.2210 (13)	0.109 (1)

There is one anomaly of the lattice parameters visible at 242 K (on cooling), which corresponds to the phase transition to the ferroelectric phase (Jakubas, 1986). In the temperature dependence of the a parameter there is an anomaly visible of the change in slope at T_c, while the temperature dependence of β does not show any anomaly in the vicinity of T_c. The decrease in the a parameter reflects the decrease in distances between the polyanionic layers.

In the temperature dependence of b and c parameters the transition is clearly visible. The changes of the lattice parameters in the bc polyanionic layer are smaller than in the a direction. It should be noted that the change in length of the c parameter is ca four times larger than that of b. The changes in the signs of the slopes of the b and c parameters at T_c reflect the changes in hydrogen bonding at the transition temperature.

The volume of the unit cell can be well approximated by a straight line about 242 K and by a second-order polynomial below 242 K. There is no discontinuity in the volume at the phase transition, as expected for a second-order phase transition; the values of dV/dt are essentially equal both above and below T_c.*

The phase transition at 242 K to the ferroelectric phase was attributed to ordering of one of two non-equivalent dimethylammonium cations (Gdaniec, Kosturkiewicz, Jakubas & Sobczyk, 1988). Above T_c it was suggested that the dimethylammonium cation located inside the polyanionic cavity reorients along the axis comprising C atoms, between two positions, while below T_c its reorientations are frozen. This leads to the appearance of a spontaneous polarization. The application of an external electric field would lead to switching of this cation between two possible positions.

Our investigation of the structure of DMACA at 200 and 298 K generally seems to confirm this mechanism with the modification that the rotation axis does not comprise the C atoms, but is parallel to them and passes through the centre of gravity of the molecule. In the ferroelectric phase the N(1) cation was ordered, while in the paraelectric phase it is disordered by splitting the N and C atoms between two positions with the site occupancy factor 0.5.

The difference-Fourier map for the cation located inside the polyanionic cavity at 298 K is presented in Fig. 6. The figure plane is perpendicular to the axis along which reorientations occur and comprise disordered N(1)

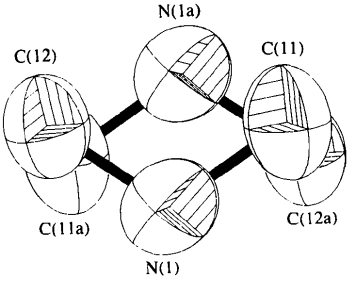

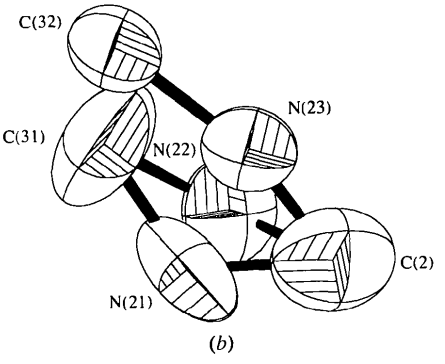

Fig. 4. Disordered dimethylammonium cations (*a*) N(1) and (*b*) N(2) at 298 K.

* Lists of structure factors, anisotropic displacement parameters, H-atom coordinates and complete geometry, and Figs. 1*S* and 2*S* have been deposited with the IUCr (Reference: HR0024). Copies may be obtained through The Managing Editor, International Union of Crystallography, 5 Abbey Square, Chester CH1 2HU, England.

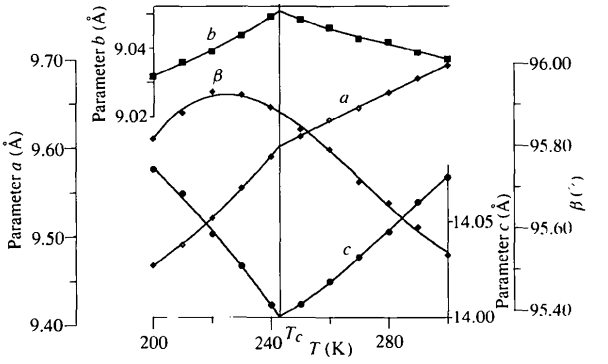

Fig. 5. The temperature dependencies of the a, b, c and β lattice parameters of DMACA.

and N(1a) atoms. The additional electron density in the intermediate positions suggests that the reorientation of this cation in the paraelectric phase occurs between not two, but actually four positions, similar to the recently studied $[NH_2(CH_3)_2]Al(SO_4)_2.6H_2O$ crystal (Pietraszko, Łukaszewicz & Kirpichnikova, 1993). It seems, however, evident that close to room temperature two of the potential wells are much deeper than the other two, so that the cation after each reorientation spends most of the time in the deeper wells. [Attempts at splitting N(1) were not successful, leading to very large values of U_{22} for the N atom placed in the position of additional electron density.]

At 298 K the cation located inside the polyanionic layer, N(1), is disordered, having two positions for N and C atoms, while that located between the polyanionic layers, N(2), has three positions for N atoms and two for one of the C atoms. At 200 K in the ferroelectric phase the cation located inside the polyanionic layer, N(1), is ordered, while that of one of the two non-equivalent cations located between the layers, N(2), is ordered and the other, N(3), is disordered by splitting the N and C atoms between two positions.

This indicates that the cation located inside the polyanionic cavity, at a given temperature, possesses a smaller degree of rotational freedom than the cations located between the polyanionic layers. The reorientational motions of the cation located inside the polyanionic cavity are frozen at T_c, while freezing reorientations of cations located between polyanionic layers occurs at lower temperature. At 200 K one of three crystallographically non-equivalent cations still reorients.

The critical slowing down of the relaxation frequency close to T_c, observed in dielectric dispersion studies (Bator & Jakubas, 1995), and the results of present X-ray studies corroborate the order–disorder mechanism of the ferro-paraelectric phase transition connected with ordering the dimethylammonium cation located inside the polyanionic cavity.

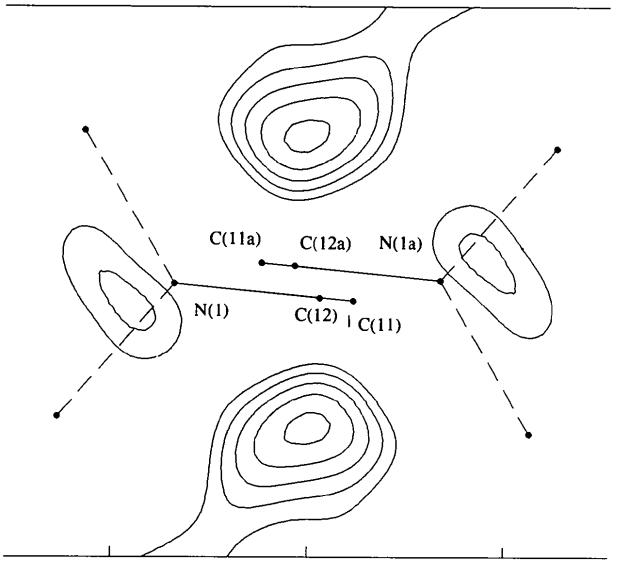

Fig. 6. Difference electron-density contours (0.2, 0.3, 0.4, 0.5 and 0.6 e Å^{-3}) of the N(1) disordered cation at 298 K. C(11) and C(12) atoms are above and below the figure plane. Additional electron density suggests that the reorientations of the N(1) cation occur between not two, but actually four positions.

3.3. *Influence of hydrogen bonds on the distortion of octahedral coordination of the Sb atom*

It is interesting to note that the polyanionic sublattice of DMACA is markedly distorted, the Sb—Cl bond lengths differing significantly from each other. The Sb—Cl lengths at 200 K involving terminal chlorines are between 2.393 and 2.617 Å, and those involving bridging chlorines are between 2.625 and 3.247 Å. At 298 K the Sb—Cl lengths involving terminal chlorines are between 2.409 and 2.501 Å, while for bridging chlorines between 2.819 and 3.112 Å.

In a similar compound, $[C(NH_2)_3]_3Sb_2Cl_9.0.9H_2O$, tris(guanidinium) nonachlorodiantimonate hydrate (GNCA), it was found to possess an almost non-deformed polyanionic sublattice. In GNCA the values of the Sb—Cl bond lengths are equal to 2.452 Å for bonds involving terminal chlorines and 2.946 Å for bonds involving bridging chlorines, each short bond being opposite a long one (Zaleski & Pietraszko, 1994).

It should be noted that in the case of DMACA the Sb—Cl bond lengths are significantly different from that characteristic of a non-deformed lattice. Similar differences in Sb—X bond lengths were found in all other halogenoantimonates and bismuthates. From a comparison of the dependence of Sb—Cl bond lengths on the presence and strength of N—H···Cl hydrogen bonds we notice that the distortion of Sb—Cl contacts of the mean values characteristic of terminal and bridging chlorines and deformation of Cl—Sb—Cl angles from 90° can be explained by the presence of N—H···Cl hydrogen bonds. The influence of hydrogen bonds on Bi—Cl bond lengths was observed, *e.g.* by Lazarini (1987) and Jarraya, Ben Salah, Daoud, Rothammel & Burzlaff (1993).

The shortest N···Cl contacts in GNCA are 3.36–3.41 Å. They do not distort Sb—Cl bond lengths, but result in a weak deformation of Cl—Sb—Cl angles from 90°. The hydrogen bonds with Cl···N contacts larger than 3.50 Å do not lead to any deformation of the octahedral coordination of the Sb atom.

Appropriate Sb—Cl bond lengths in DMACA at 298 K and 200 K are given in Table 5. To this we added the bonds formed by a closely related compound, tris(trimethylammonium) nonachlorodiantimonate $[NH(CH_3)_3]_3Sb_2Cl_9$ (TMACA), which crystallizes with the same polyanionic sublattice (at 296 K in ferroelectric

Table 5. *Comparison of lengths of Sb—Cl bonds for DMACA at 200 and 298 K and for TMACA at 296 K*

Bonds in a given row are equivalent (despite a different numbering scheme) for the three structures. To help to take into account the *trans* effect the bonds in rows 1, 2 and 3 are opposite bonds located in rows 4, 5 and 6, respectively.

	DMACA (200 K)		DMACA (200 K)		DMACA (298 K)		DMACA (298 K)
Sb(1)—Cl(2)	2.405 (2)	Sb(2)—Cl(7^{i})	2.617 (2)	Sb(1)—Cl(1)	2.409 (2)		
Sb(1)—Cl(6)	2.587 (2)	Sb(2)—Cl(5)	2.393 (2)	Sb(1)—Cl(2)	2.458 (2)		
Sb(1)—Cl(3)	2.447 (2)	Sb(2)—Cl(1)	2.409 (2)	Sb(1)—Cl(3)	2.501 (2)		
Sb(1)—Cl(8)	3.199 (2)	Sb(2)—Cl(8)	2.625 (2)	Sb(1)—Cl(4^{iii})	3.112 (2)	Cl(4^{iii})—Sb(1^{iii})	2.819 (2)
Sb(1)—Cl(9^{i})	2.691 (2)	Sb(2)—Cl(9)	3.247 (2)	Sb(1)—Cl(5)	2.926 (2)	Cl(5)—Sb(1^{iv})	2.926 (2)
Sb(1)—Cl(4)	2.905 (2)	Sb(2)—Cl(4^{ii})	3.088 (2)	Sb(1)—Cl(4)	2.819 (2)	Cl(4)—Sb(1^{v})	3.112 (2)

Symmetry codes: (i) $x, 1-y, z-\frac{1}{2}$; (ii) $x, 1+y, z$; (iii) $1-x, -\frac{1}{2}+y, \frac{1}{2}-z$; (iv) $1-x, -y, -z$; (v) $1-x, \frac{1}{2}+y, \frac{1}{2}-z$.

phase, in *Pc* space group).* To make this comparison easier, during the structure solution of DMACA at 200 K, we used the same origin for the coordinate system and have adopted the same atomic numbering scheme of Sb and Cl atoms as that of TMACA (Kallel & Bats, 1985). For a discussion of these dependences we grouped the hydrogen bonds present in DMACA at 200 and 298 K and in TMACA at 296 K in Table 6.

In comparing the Sb—Cl bond lengths a *trans* effect has to be taken into account. The elongation of any particular Sb—Cl bond leads to a shortening of the Sb—Cl distance located opposite.

Comparing Sb—Cl lengths in DMACA at 298 K we notice that only one N···Cl contact is smaller than 3.4 Å [N(22)—H(22*B*)···Cl(4) = 3.29 (1) Å]. Only this hydrogen bond distorts the octahedral coordination of the Sb atom. The Cl(4) atom is shifted from its central position between Sb atoms, leading to elongation of the Sb(1)—Cl(4‴) bond and shortening of Sb(1^{III})—Cl(4‴). The second bridging chlorine is situated in the geometrical centre between Sb atoms, with Sb(1)—Cl(5) 2.926 (2) Å (close to a non-deformed value). The Cl(2) atom situated *trans* to Cl(5) shows an Sb(1)—Cl(2) distance of 2.458 (2) Å, close to the non-deformed terminal Sb—Cl length in GNCA.

An increase in Sb(1)—Cl(4‴) length to 3.112 (2) Å leads to a shortening of the opposite Sb(1)—Cl(1) bond to 2.409 (2) Å, on the other hand, shortening the Sb(1^{III})—Cl(4‴) bond to 2.819 (2) Å results in elongation of the opposite Sb(1)—Cl(3) bond to 2.501 (2) Å.

At 200 K there are six Cl···N contacts shorter than 3.4 Å. They form hydrogen bonds involving Cl(4), Cl(6), Cl(9) and Cl(7). The Sb—Cl bond lengths involving terminal chlorines are generally close to a mean value of 2.45 Å, with the exception of Sb(1)—Cl(6) and Sb(2)—Cl(7) which are much larger. The hydrogen bonds formed by Sb(1)—Cl(6) are presented in Fig. 7. There are two hydrogen bonds situated on each side of Cl(6): N(31)—H(31*A*)···Cl(6) and N(1)—H(1*A*)···Cl(6). They elongate the Sb(1)—Cl(6) bond to 2.587 (2) Å. A similar situation is found for Sb(2)—Cl(7).

Comparing the lengths of the Sb—Cl bonds involving bridging chlorines reveals that, with the exception of Sb(1)—Cl(5)—Sb(1a) for DMACA at 298 K which has two equal Sb—Cl contacts, in all other cases the Cl atoms are located outside the centre between two Sb atoms.

Fig. 8 presents the Sb(1)—Cl(5)—Sb(1a) bonds at 298 K in the paraelectric phase and at 200 K in the ferroelectric phase (at 200 K we have a different atomic numbering scheme, but the atoms are the same). It should be noted that in the paraelectric phase Cl(5) does not take part in hydrogen bonding, whereas in the ferroelectric phase a moderately strong N(2)—H(2*A*)···Cl(9) hydrogen bond occurs, as a result of which the Cl(9) atom is displaced in the direction of the N(2) atom. The Sb(1a)—Cl(5)—Sb(1) angle is 180° at 298 K and 165.4° at 200 K, which proves the shift of Cl(9).

In the case of TMACA, which forms an even stronger N(2)—H(2*A*)···Cl(9) bond (*cf.* Table 6), this angle is equal to 160.1°. It should be noted that the increase in the Sb—Cl mean bond lengths involving the Cl atom in

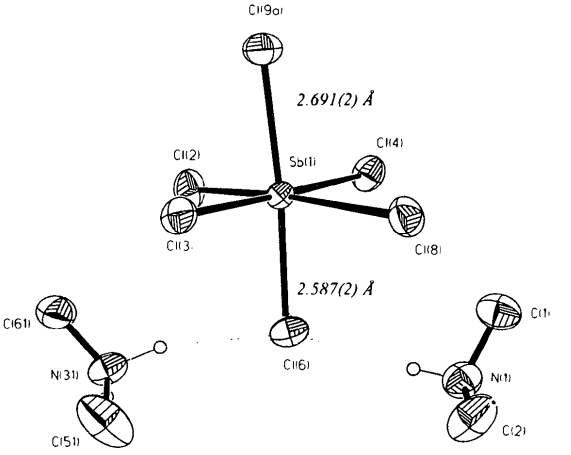

Fig. 7. Scheme of hydrogen bonding involving the Cl(6) atom at 200 K, resulting in elongation of the Sb(1)—C(6) bond from a mean value of 2.45 Å to a value of 2.587 Å.

* See diagram of TMACA structure in deposited material (see footnote to p. 291).

Table 6. *Hydrogen-bond geometries* for DMACA at 200 and 298 K and TMACA at 296 K*

D—H···*A*	*D*···H	H—*A*	*D*···*A*	*D*—H···*A*
DMACA at 200 K				
N(1)—H(1*A*)···Cl(6^{i})	0.98 (3)	2.46 (4)	3.34 (1)	150 (3)
N(1)—H(1*B*)···Cl(4)	0.82 (3)	2.45 (4)	3.25 (1)	162 (3)
N(2)—H(2*A*)···Cl(9)	0.92 (3)	2.39 (3)	3.28 (1)	163 (3)
N(2)—H(2*B*)···Cl(7^{ii})	0.91 (3)	2.40 (4)	3.30 (1)	171 (3)
N(31)—H(31*A*)···Cl(6^{iii})	0.97 (3)	2.47 (3)	3.39 (1)	157 (3)
N(31)—H(31*B*)···Cl(7^{iv})	0.82 (3)	2.47 (3)	3.18 (1)	146 (3)
DMACA at 298 K				
N(1)—H(1*A*)···Cl(2)	0.90	2.63	3.49 (1)	162 (3)
N(1)—H(1*B*)···Cl(4^{v})	0.90	2.66	3.48 (1)	151 (3)
N(21)—H(21*A*)···Cl(3^{vi})	0.90	2.58	3.46 (2)	168 (3)
N(22)—H(22*B*)···Cl(4^{vii})	0.90	2.41	3.29 (1)	167 (3)
N(23)—H(23*A*)···Cl(4^{vii})	0.90	2.69	3.56 (1)	161 (3)
TMACA at 296 K				
N(1)—H(1*A*)···Cl(8)	0.90	2.34	3.22 (1)	167 (3)
N(2)—H(2*A*)···Cl(9)	0.90	2.37	3.25 (1)	167 (3)
N(3)—H(3*A*)···Cl(2)	0.90	2.93	3.46 (1)	131 (1)
N(3)—H(3*A*)···Cl(4)	0.90	2.69	3.59 (1)	144 (3)

Symmetry codes: (i) $x, -y, z-\frac{1}{2}$; (ii) $x-1, y, z$: (iii) $x+1, 1-y, z+\frac{1}{2}$; (iv) $x, 2-y, z+\frac{1}{2}$; (v) $x, \frac{1}{2}-y, \frac{1}{2}+z$; (vi) $-x, \frac{1}{2}+y, \frac{1}{2}-z$; (vii) $1-x, \frac{1}{2}+y, \frac{1}{2}-z$.

question (2.926 Å at 298 K, 2.969 Å at 200 K for DMACA and 3.028 Å for TMACA at 296 K) also reflects the increase in the distortion of Sb coordination with an increase in strength of the hydrogen bonds. Table 7 presents values of Sb—Cl—Sb angles and mean values of Sb—Cl bonds involving bridging chlorines for DMACA at 200 and 298 K and for TMACA at 296 K.

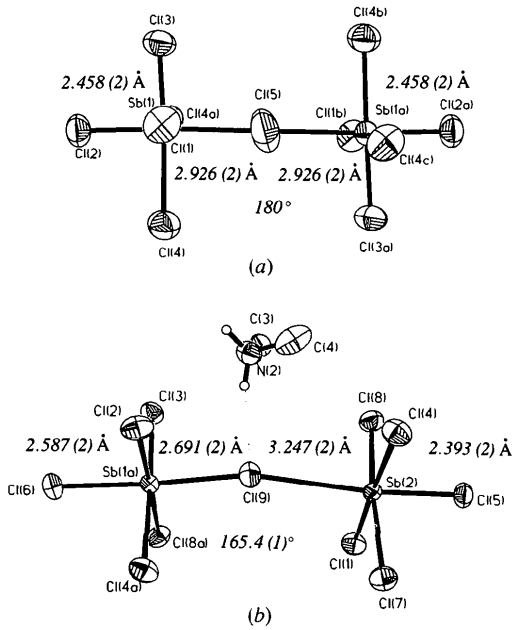

Fig. 8. Scheme of hydrogen bonding involving the bridging Cl(5) atom at (*a*) 298 and (*b*) 200 K (a different numbering scheme is used at 200 and 298 K, but the atoms are the same). In the absence of hydrogen bonds Cl(5) is in the centre between Sb(1) and Sb(1a), with the Sb(1)—Cl(5)—Sb(1a) angle equal to 180°. At 200 K in the presence of the N(2)—H(2*A*)···Cl(9) hydrogen bond, the Cl atom is displaced from its position, with the Sb(1)—Cl(9)—Sb(2) angle equal to 165.4°.

It should be noted that the mean values of Sb—Cl bond lengths for DMACA at 298 K for terminal Cl atoms, $(2.409+2.458+2.501)/3 = 2.456$, and for bridging chlorines, $(2.819+3.112+2.926)/3 = 2.952$, are close to those characteristic of the non-deformed polyanionic lattice.

Comparing the Sb—Cl bond lengths of DMACA at 298 and 200 K indicates that on decreasing temperature an increase in deformation of the polyanionic sublattice occurs. It may be connected with the increase in strength of N—H···Cl hydrogen bonds. At room temperature DMA cations reorientate and are attracted to anions by merely Coulomb interactions. On decreasing the temperature the reorientations of the cations freeze, which as a result led to a situation where they are connected to the anionic sublattice by Coulomb interactions as well as by hydrogen bonds.

The deformation of octahedral coordination of antimony(III) may be connected with the presence of a lone-electron pair on the Sb atom. In the majority of alkylammonium halogenoantimonates the lone-electron pair is stereochemically inactive. In the case of isolated $SbCl_6^{3-}$ octahedra, with a lack of strong electrostatic interactions and the presence of hydrogen bonds, the Sb—Cl bond lengths are equal to each other. It may be explained by assuming that the lone pair occupies the orbital of a spherical symmetry (type *s*). This leads to an increase in Sb—Cl bond lengths compared with the Sb—Cl lengths of pentavalent antimony, $Sb^{III}—Cl = 2.65$, $Sb^{V}—Cl = 2.38$ Å (Prassides, Day & Cheetham, 1985). It should be noted that the lone-electron pair may be easily deformed from spherical symmetry. This takes place either due to the presence of packing forces, the formation of Sb—*X*—Sb bonds, electrostatic Colomb interactions or the formation of hydrogen bonds. In the case of DMACA the polyanionic vacancies are large enough so that DMA cations easily fit inside (packing interactions may be neglected). The electric charge is well diffused on cations. The presence of Sb—Cl—Sb bonds result in the deformation of the lone pair of electrons on Sb from spherical symmetry, resulting in two clearly defined bond lengths of 2.45 Å for terminal and 2.95 Å for bridging chlorines. Further deformation of the lone pair may occur by the formation of N—H···Cl hydrogen bonds, as proven in this work.

4. Conclusions

DMACA undergoes a second-order phase transition at 242 K, connected with a critical slowing down of reorientations of dimethylammonium cations located inside the polyanionic cavities at T_c.

Cations placed between the polyanionic layers possess larger reorientational freedom and are frozen at lower

Table 7. *Comparison of angles and mean values of lengths of bonds involving bridging Cl atoms in DMACA at 200 and 298 K and in TMACA at 296 K*

Atom labelling for DMACA at 200 K and TMACA at 296 K

	Angles			Mean values Sb—Cl bond lengths		
	DMACA 298 K	DMACA 200 K	TMACA 296 K	DMACA 298 K	DMACA 200 K	TMACA 296 K
Sb(1)—Cl(4)—Sb(2^{i})	163.9	157.0	163.0	2.966	2.997	3.072
Sb(1)—Cl(8)—Sb(2)	163.9	167.3	157.6	2.966	2.912	3.100
Sb(1)—Sl(9^{ii})—Sb(2^{ii})	180	165.4	160.1	2.926	2.969	3.028

Symmetry codes: (i) $x,\ y-1,\ z$; (ii) $x,\ 1-y,\ z-\frac{1}{2}$.

temperatures. At 200 K one of non-equivalent cations still reorients.

Freezing of the reorientations of cations led to the formation of stronger N—H···Cl hydrogen bonds, which result in deformation of the polyanionic sublattice. This is probably connected with a deformation of the lone-electron pair on the antimony(III) atom.

The authors are grateful to Professor Z Gałdecki (Technical University of Łódź, Poland) for allowing the use of the Siemens *SHELXTL/PC* program system in his laboratory.

References

Aurivillius, B. & Stalhandske, C. (1978). *Acta Chem. Scand. A*, pp. 715–719.
Bator, G. & Jakubas, R. (1995). *Phys. Status Solidi A*, **147**, 591–600.
Chabot, B. & Parthe, E. (1978). *Acta Cryst.* B**34**, 645–648.
Galewski, Z., Jakubas, R. & Sobczyk, L. (1990). *Acta Phys. Pol. A*, **78**, 645–650.
Gdaniec, M., Kosturkiewicz, Z., Jakubas, R. & Sobczyk, L. (1988). *Ferroelectrics*, **77**, 31–37.
Hall, M., Nunn, M., Begley, M. J. & Sowerby, D. B. (1986). *J. Chem. Soc. Dalton Trans.* pp. 1231–1238.
Jakubas, R. (1986). *Solid State Commun.* **60**(4), 389–391.
Jakubas, R. & Sobczyk, L. (1990). *Phase Transit.* **20**, 163–193.
Jakubas, R., Czapla, Z., Galewski, Z. & Sobczyk, L. (1986). *Ferroelectr. Lett.* **5**, 143–148.
Jakubas, R., Czapla, Z., Galewski, Z., Sobczyk, L., Żogał, O. J. & Lis, T. (1986). *Phys. Status Solidi A*, **93**(2), 449–455.
Jakubas, R., Malarski, Z. & Sobczyk, L. (1988). *Ferroelectrics*, **80**, 193–196.
Jakubas, R., Sobczyk, L. & Matuszewski, J. (1987). *Ferroelectrics*, **74**, 339–345.
Jarraya, S., Ben Salah, A., Daoud, A., Rothammel, W. & Burzlaff, H. (1993). *Acta Cryst.* C**49**, 1594–1596.
Kallel, A. & Bats, J. W. (1985). *Acta Cryst.* C**41**, 1022–1024.
Kihara, K. & Sudo, T. (1971). *Z. Kristallogr.* **134**, 142–144.
Lazarini, F. (1977). *Acta Cryst.* B**33**, 2961–2964.
Lazarini, F. (1987). *Acta Cryst.* C**43**, 637–638.
Miniewicz, A. & Jakubas, R. (1987). *Solid State Commun.* **63**(10), 933–936.
Miniewicz, A., Lefebvre, J. & Jakubas, R. J. (1991). *Raman Spectrosc.* **22**, 435–443.
Pietraszko, A., Łukaszewicz, K. & Kirpichnikova, L. F. (1993). *Polish J. Chem.* **67**, 1877–1884.
Prassides, K., Day, P. & Cheetham, A. K. (1985). *Inorg. Chem.* **24**, 545–552.
Sheldrick, G. M. (1990). *SHELXTL/PC User's Manual.* Siemens Analytical X-ray Instruments Inc., Madison, Wisconsin, USA.
Zaleski, J. & Pietraszko, A. (1994). *Z. Naturforsch. Teil A*, **49**(9), 895–901.